Fr_P03_14

Working around the Corner Problem in Numerically Exact Non-Reflecting Boundary Conditions for the Wave Equation

W.A. Mulder[1,2]*

[1] Shell Global Solutions International BV; [2] Delft University of Technology

Summary

Recently introduced non-reflecting boundary conditions are numerically exact: the solution on a given domain is the same as a subset of one on an enlarged domain where boundary reflections do not have time to reach the original domain. In 1D with second- or higher-order finite differences, a recurrence relation based on translation invariance provides the boundary conditions. In 2D or 3D, a recurrence relation was only found for a non-reflecting boundary on one or two opposing sides of the domain and zero Dirichlet or Neumann boundaries elsewhere. Otherwise, corners cause translation invariance to be lost.

The proposed workaround restores translation invariance with classic, approximately non-reflecting boundary conditions on the other sides. As a proof of principle, the method is applied to the 2-D constant-density acoustic wave equation, discretized on a rectangular domain with a second-order finite-difference scheme, first-order Enquist-Majda boundary conditions as approximate ones, and numerically exact boundary conditions in the horizontal direction. The method is computationally costly but has the advantage that it can be reused on a sequence of problems as long as the time step and the sound speed values next to the boundary are kept fixed.

Introduction

Modelling seismic wave propagation in a subset of the Earth requires truncation of the computational domain to the region of interest. The resulting artificial boundaries should not create reflections that were absent in the original problem. The large number of papers on the subject suggests that this can not be considered a solved problem.

Numerically exact non-reflecting boundary conditions produce a solution that is the same as a subset of one obtained on an enlarged domain with boundaries moved so far away that their reflections do not have time to reach the original domain (Mulder, 2019). In that sense, they differ from perfectly matched layers (Berenger, 1994) or the exact conditions of Ting and Miksis (1986) that exploit Green's second identity. Givoli and Cohen (1995) showed that the latter suffer from a weak instability that can be suppressed by adding some dissipation. Teng (2003) proposed a formulation based on boundary integrals, which after discretization becomes the local condition of Engquist and Majda (1979).

The numerically exact non-reflecting boundary conditions are based on the boundary Green functions computed for the discretized partial differential equation. In the one-dimensional case with a finite-difference approximation of second or higher order, the boundary conditions obey a recurrence relation. In the generalization to more than one space dimension and with a rectangular domain, the derivation of a recurrence relation seems only to be feasible for a single non-reflecting boundary, or for two of them at opposing ends of the domain. The other boundaries should then be zero Dirichlet or Neumann. The reason is the assumed translation invariance in the direction perpendicular to the boundary. This property is lost in the presence of a corner where two non-reflecting boundaries meet.

The workaround proposed here combines the exact boundary condition in one coordinate direction with a classic, approximately non-reflecting boundary condition (Engquist and Majda, 1979; Higdon, 1986, a.o.) in the other coordinate direction(s). This restores translation invariance at the expense of numerical exactness. Still, the method can be useful if the approximately non-reflecting boundary conditions produce too strong unwanted reflections in one coordinate direction. This can happen, for instance, when modelling interbed multiples in marine examples with a shallow sea or in land examples with strong surface waves.

The method is described for the simplest case of the 2-D constant-density acoustic wave equation discretized with the lowest-order finite-difference scheme. Numerical tests are included.

Method

The constant-density acoustic wave equation in 2D is given by

$$\frac{1}{c^2}\frac{\partial^2 u}{\partial t^2} = \frac{\partial^2 u}{\partial x^2} + \frac{\partial^2 u}{\partial z^2} + f, \tag{1}$$

with a solution $u(t,x,z)$ depending on time t and position (x,z) in a given sound speed model $c(x,z)$ for a source term $f(t,x,z)$ typically of the form $w(t)\delta(x-x_s)\delta(z-z_s)$ for a point source at (x_s,z_s) with wavelet $w(t)$. The rectangular computational domain is defined by $[x_{\min},x_{\max}]\times[z_{\min},z_{\max}]$ and discretized on a grid with $N_x \times N_z$ points: $x_i = x_{\min} + (i-\frac{1}{2})\Delta x$, $i = 1,\ldots,N_x$, and $z_j = z_{\min} + (i-\frac{1}{2})\Delta z$, $i = 1,\ldots,N_z$, with grid spacings $\Delta x = (x_{\max} - x_{\min})/N_x$ and $\Delta z = (z_{\max} - z_{\min})/N_z$, respectively. The standard second-order finite-difference scheme in space and time is

$$\frac{1}{c_{i,j}^2 \Delta t^2}\left(u_{i,j}^{n+1} - 2u_{i,j}^n + u_{i,j}^{n-1}\right) = \frac{1}{\Delta x^2}\left(u_{i+1,j}^n - 2u_{i,j}^n + u_{i-1,j}^n\right) + \frac{1}{\Delta z^2}\left(u_{i,j+1}^n - 2u_{i,j}^n + u_{i,j-1}^n\right) + f_{i,j}^n. \tag{2}$$

Time is discretized by $t^n = t^0 + n\Delta t$ with a constant time step Δt that should obey the CFL stability limit $\Delta t\sqrt{(\Delta x)^{-2} + (\Delta z)^{-2}}\,\max_{i,j}(c_{i,j}) \le 1$.

In the example in the next section, a free-surface boundary condition is imposed at $z_{\min} = 0$ and the other boundaries should be non-reflecting. At $z_{\max}$, the lowest-order Engquist and Majda (1979) boundary

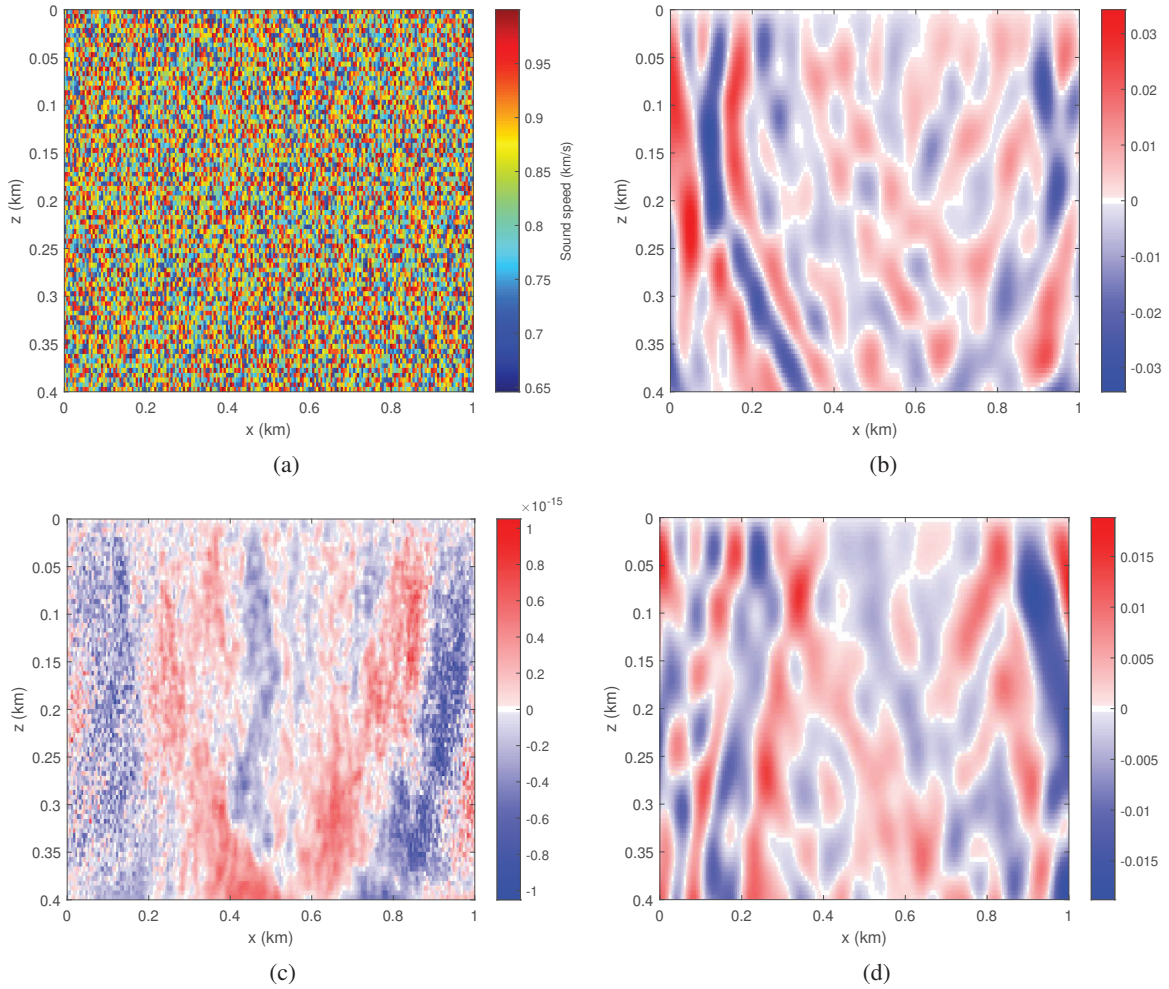

Figure 1 *(a) Random sound speed model. (b) Wave field after 2 s for the exact non-reflecting boundaries at the left and right and the Enquist-Majda boundary condition at the bottom. (c) Difference between the wavefield from (b) and one modelled on a domain enlarged at the left and right, but with the Enquist-Majda boundary condition at the bottom, showing accumulated numerical round-off errors. (d) Difference between this wavefield and one modelled on an enlarged domain.*

condition, their equation (4.2), is imposed:

$$u^{n+1}_{i,j+1} = u^{n}_{i,j} + \alpha_{i,j}(u^{n}_{i,j+1} - u^{n+1}_{i,j}), \quad \text{for } j = N_z, \tag{3}$$

where $\alpha_{i,j} = (1 - \nu_{i,j})/(1 + \nu_{i,j})$ and $\nu_{i,j} = c_{i,j}\Delta t/\Delta y$. This represents a second-order implicit time discretization of the equation $\partial u/\partial t = c\,\partial u/\partial x$.

The boundary conditions at $x_{\min}$ and $x_{\max}$ are numerically exact. Only the one at $x = x_{\max}$ is reviewed, since the other follows in a similar way. The boundary Green functions $G^{n}_{N_x,j_0;i,j}$ are defined as the wavefield generated by a unit spike at time zero ($n = 0$) and position (x_{N_x}, z_{j_0}), evaluated at later time t^n, $n > 0$, and position (x_i, z_j), $i > N_x$, while setting the wavefield to zero at $x = x_{N_x}$ for $n > 0$. This means that $G^{n}_{N_x,j_0;N_x,j} = \delta_{j,j_0}\delta_{n,0}$, using the Kronecker delta. With these Green functions, the wavefield just outside the domain can be predicted from earlier values on the boundary:

$$u^{n}_{N_x+1,j} = \sum_{m=1}^{n}\sum_{j_0=1}^{N_z} u^{n-m}_{N_x,j_0}\, G^{m}_{N_x,j_0;N_x+1,j}. \tag{4}$$

Note that this expression only holds for the lowest-order discretization. For higher orders, additional points for some values of $i < N_x$ are involved.

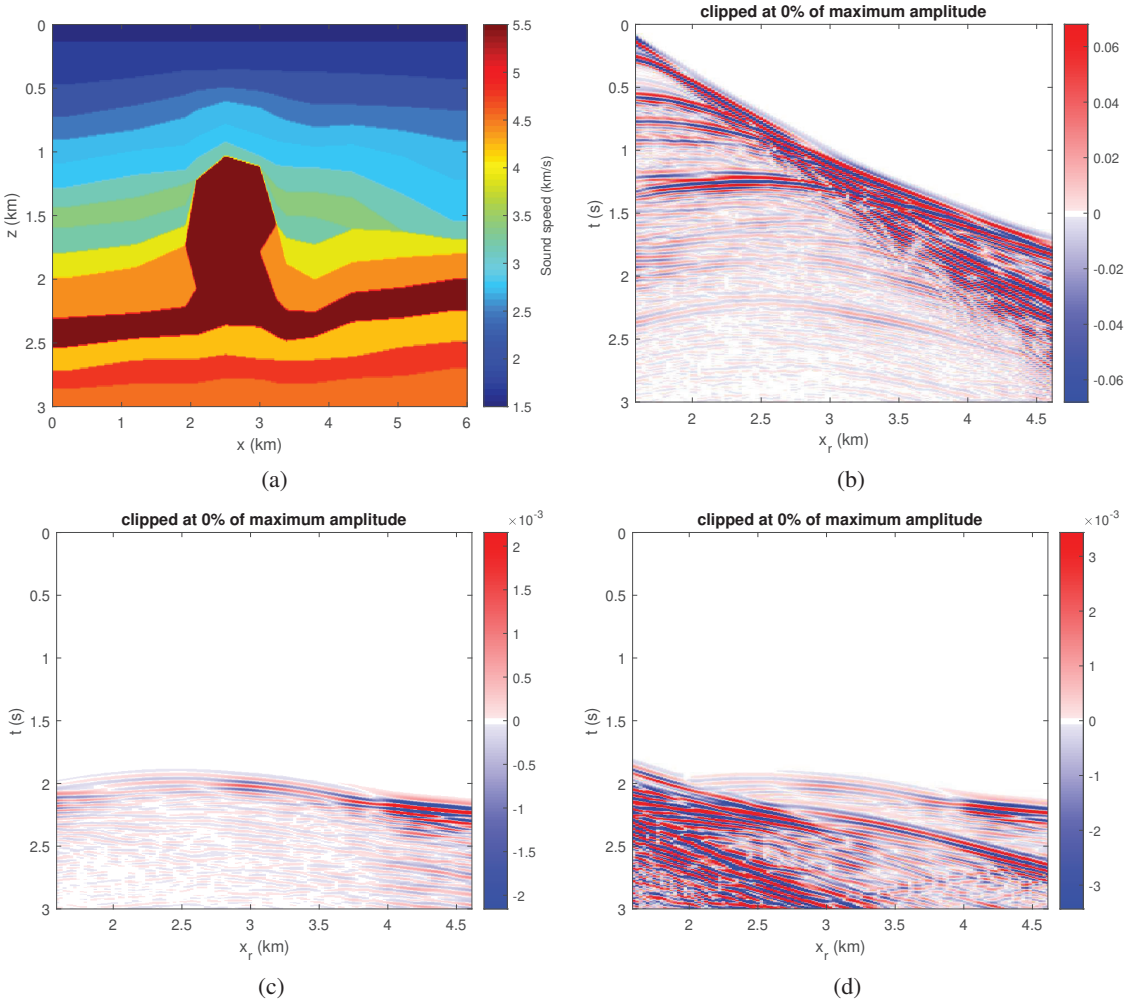

Figure 2 *(a) Sound speed model. (b) Seismogram. (c) Difference between the seismogram displayed in (b) and one obtained on an enlarged domain, showing only reflections from the bottom. (d) Difference between a seismogram for Enquist-Majda conditions at all sides except the free surface and one obtained on the enlarged domain.*

The boundary Green functions $G^n_{N_x,j_0;i,j}$ at $i = N_x + 1$ follow from the discrete wave equation (2) with zero source term $f^n_{i,j} = 0$. Constant extrapolation in the direction perpendicular to the boundary is applied to the sound speed: $c_{i,j} = c_{N_x,j}$ for $i > N_x$. Initially, $G^0_{N_x,j_0;N_x+1,j} = 0$ and $G^1_{N_x,j_0;N_x+1,j} = (c_{N_x,j}\Delta t/\Delta x)^2\delta_{j_0,j}$. The boundary at the free surface can be modelled by anti-symmetric extrapolation: $G^n_{N_x,j_0;N_x+1,0} = -G^n_{N_x,j_0;N_x+1,1}$. At the bottom ($j = N_z$), the Enquist-Majda condition furnishes the extrapolated values $G^n_{N_x,j_0;N_x+1,N_z+1}$. At the left ($i = N_z$), all values are zero except for time $n = 0$. At the right ($i = N_z + 2$), equation (4) provides

$$G^n_{N_x,j_0;N_x+2,j} = \sum_{m=1}^{n-1}\sum_{k=1}^{N_z} G^m_{N_x,j_0;N_x+1,k}\,G^{n-m}_{N_x,k;N_x+1,j}, \quad n > 1. \tag{5}$$

Its earlier values are zero. Note that the last equation assumes translation invariance in the direction perpendicular to the boundary.

Results

As a proof of principle, the random velocity model shown in Figure 1a is considered with a source placed at $x_s = 400\,\mathrm{m}$ and $z_s = 100\,\mathrm{m}$ and a wavelet $w(t) = -\frac{\mathrm{d}}{\mathrm{d}t}[4(t/T_w)(1-t/T_w)]^{12}$ for $0 \le t \le T_w = 0.325\,\mathrm{s}$

and zero otherwise. The grid spacing is $\Delta x = \Delta z = 5\,\mathrm{m}$. A free-surface boundary condition is present at $z_{\min} = 0\,\mathrm{m}$. Figure 1b displays the wavefield after 2 s. Figure 1c shows the difference of the wavefield with one computed on a domain that is enlarged at $x_{\min}$ and $x_{\max}$ to avoid any boundary reflections but uses the Enquist-Majda condition at $z_{\max}$. The sound speed in the enlarged domain is obtained by constant extrapolation in the direction perpendicular to the boundary. If this is performed in sequence per coordinate, corner values are dealt with automatically. The effectiveness of the exact boundary conditions is obvious: only accumulated numerical round-off errors are visible. The comparison to a solution on a domain that is also enlarged at $y_{\max}$ shows the result of boundary reflection at the bottom, caused by the approximate character of the Enquist-Majda condition.

Figure 2a shows a velocity model for a second example of a salt diapir in a marine environment with a shallow sea. A seismogram for a shot at $x_s = 1495\,\mathrm{m}$ and $z_s = 5\,\mathrm{m}$ is displayed in Figure 2b, for the same wavelet as in the previous example but now with $T_w = 1.625/f_{\mathrm{peak}}$, $f_{\mathrm{peak}} = 12\,\mathrm{Hz}$. Receivers were placed at a depth of 10 m between $x_r = 1600$ and 4600 m at a 25-m interval. The grid spacing was 10 m. Figure 2c shows the difference between this seismogram and one computed on an enlarged domain. Only reflections from the bottom, caused by the approximate character of the Enquist-Majda boundary conditions, are visible. For reference, Figure 2c plots the difference between a seismogram determined with Enquist-Majda boundary conditions at all sides except the free surface and the one obtained on the enlarged domain. The reflections from the vertical boundaries stand out. This demonstrates the usefulness of the method in cases where reflections in one coordinate directions are much stronger than for the other, for instance, with the shallow sea used here, or with strong surface waves in land seismic examples.

Conclusions

Numerically exact non-reflecting boundaries in only one coordinate direction can be advantageous in the presence of a shallow water layer or with strong surface waves. The convolutions in equations (4) and (5) are the most costly part of the method. However, the boundary Green functions can be reused for a several problems as long as the grid size, time step and sound speed values next to the boundaries do not change. Higher-order finite-difference discretizations are feasible, as well as a combination with higher-order approximately non-reflecting boundary conditions.

References

Berenger, J.P. [1994] A perfectly matched layer for the absorption of electromagnetic waves. *Journal of Computational Physics*, **114**(2), 185–200.

Engquist, B. and Majda, A. [1979] Radiation boundary conditions for acoustic and elastic wave calculations. *Communications on Pure and Applied Mathematics*, **32**(3), 313–357.

Givoli, D. and Cohen, D. [1995] Nonreflecting boundary conditions based on Kirchhoff-type formulae. *Journal of Computational Physics*, **117**(1), 102–113.

Higdon, R.L. [1986] Absorbing boundary conditions for difference approximations to the multi-dimensional wave equation. *Mathematics of Computation*, **47**(176), 437–459.

Mulder, W.A. [2019] Exact non-reflecting boundary conditions with an FDTD scheme for the scalar wave equation in waveguide problems. *Progress in Electromagnetics Research*. Submitted.

Teng, Z.H. [2003] Exact boundary condition for time-dependent wave equation based on boundary integral. *Journal of Computational Physics*, **190**(2), 398–418.

Ting, L. and Miksis, M.J. [1986] Exact boundary conditions for scattering problems. *The Journal of the Acoustical Society of America*, **80**(6), 1825–1827.